Electrical and optical characterization of macroporous silicon antireflection coating for solar cells

FARUK FONTHAL[*]
IVALDO TORRES[**]

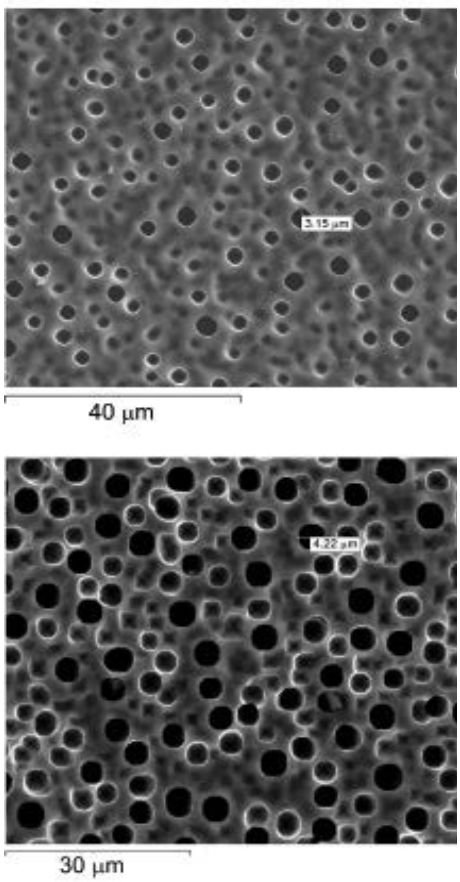

Resumen

Se ha obtenido una capa de silicio macroporoso (ma-PS) formada electroquímicamente sobre una superficie de silicio cristalino tipo n (n-Si), con el fin de mejorar la absorción óptica y desarrollar capas antirreflectoras (ARC) para celdas solares. Un modelo eléctrico fue propuesto para explicar la medición de la curva típica de corriente – voltaje (C – V). El desarrollo de las capas antirreflectivas ma-PS/n-Si fue evaluado a través de la medición de la reflectividad a 45°, en un rango de longitud de onda desde 200 a 1100 nm, obteniendo valores muy bajos del coeficiente de reflectividad (por debajo de ~10 %).

Palabras clave: silicio poroso, ataque electroquímico, capas antirreflectivas.

Abstract

Macroporous Silicon (ma-PS) on crystalline silicon type – n (n-Si)

(*) Advanced Materials for Micro and Nanotechnology Research Group - Imamnt, Universidad Autónoma de Occidente, calle 25 No. 115 - 85, Cali, 760030, Colombia.

(**) Advanced Materials for Micro and Nanotechnology Research Group - Imamnt, Universidad Autónoma de Occidente, calle 25 No. 115 - 85, Cali, 760030, Colombia. Grupo de investigación Logos, Facultad de Ingenierías y Arquitecturas, km 1 vía a Bucaramanga, Pamplona, Colombia

Reception's date: 29/11/2014 – Aceptation's date: 02/02/2015.

diodes were obtained by electrochemical etching of Si wafers, which improve the optic absorption by antireflective coatings (ARC) in solar cells. An electrical model was proposed in order to explain the measured current-voltage characteristics (I – V). The ma-PS/n-Si's performance as antireflection coating was evaluated by reflectivity measurements at 45º in the wavelength range from 200 to 1100 nm, resulting in very low reflectance values (below ~10%).

Keywords: porous silicon, electrochemical etching, antireflection coating.

1. Introduction

Macroporous silicon (ma-PS) continues to attract attention because of its potential for creating visible radiation sources and for integrating optoelectronic and microelectronics elements based on silicon technology (Ou, Zhao, Li, Diao & Wang, 2012).

The current – voltage characteristics (I – V) of the ma-PS/n-Si structure are strongly dependent on the dimensions of the pores obtained by means of an electrochemical hydrofluoric acid (HF) etching under anodic bias (Kanungo, Maji, Saha & Basu, 2009; AbdRahim, Hashim & Ali, 2011; Salman, Hassan & Omar, 2012). For this reason, the transport mechanisms involved must be studied for each specific fabrication conditions (Fonthal & Chavarria, 2012; Xiao, Wang, Bao & Funct, 2012).

In addition, the advanced optic devices incorporate surface texturization to reduce the reflection and consequently to reinforce the optic absorption. The ma-PS can be used as a single or multilayer antireflective coating for photodiodes or solar cells (Ernst et al., 2013; Chen et al., 2015), but ma-PS/n-Si structures show different optic behavior in the optic absorption and reflectance properties, depending on the fabrication conditions.

In this paper, we focus on the electrical and optical properties of metal/ma-PS/n-Si/Al with three different ma-PS layers. First, the fabrication technique adopted to produce ma-PS surfaces is described. Second, the dark I – V characteristic of metal/ma-PS/n-Si/Al diode was measured with two different metal contacts: Silver paint and Aluminum-silver paste. Finally, in order to study the uniformity of the samples, the normalized reflectivity was measured in the ultraviolet (UV) - visible - infrared (IR) range.

2. Experiment

The samples were made of 350 µm-thick n-type silicon wafers with <100> orientation and an average resistivity of 1-10 Ω.cm.

The ma-PS layer, covering one side of the wafer, was formed by electrochemical etching in aqueous hydrofluoric acid (HF) 2,5% electrolyte. Figure 1 shows the experimental setup used for the fabrication (Fonthal, Torres & Rodríguez, 2011). The wafer is mounted on an electrochemical cell with the front side in contact with the electrolyte. The positive voltage is applied on the wafer against platinum counter electrode. The electrochemical etching takes place when electronic holes are available. In n-type silicon, the holes are minority carriers and must be generated by illumination from the backside of the wafer. Here this was achieved using a 100 W halogen lamp. The backside contact was an aluminum mesh made by 0,5 µm thick sputtering deposition, a photolithography process and a subsequent aluminum etching. For the three samples under consideration the specific fabrication conditions were kept identical, and can be found elsewhere (Fonthal et al., 2011). Only the etching time was fixed 45, 60, and 75 min.

Finally, after the electrochemical etching the wafers were cleaned in an ammoniac-fluoride corrosive mixture for 2 min at room temperature.

For the top contact, two metals were used: one was obtained depositing aluminum-silver paste (Al-Ag) over the ma-PS surface using the thick film technologies with screen printing technique and the other was obtained placing silver paint (Ag) over the ma-PS surface. An HP 4145B parameter analyzer was used to measure the dark I – V characteristic. The reflectivity measurements were performed on a SpectraPro-150i (Acton) grating spectrometer at 45º in the wavelength range from 200 to 1100 nm.

Figure 1. Electrochemical cell used for macropores fabrication

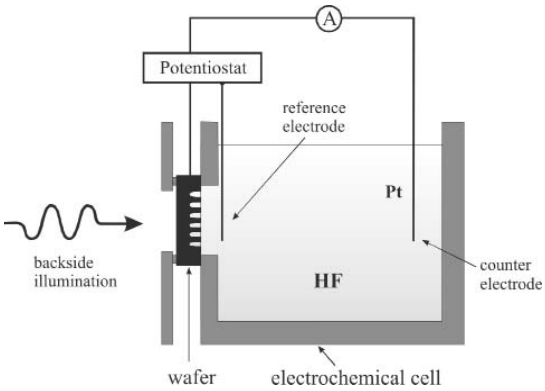

Source: by the author.

Table 1. Characteristics of the fabricated samples

Sample	J, (mA/cm2)	Etching time, (min)
A	10	45
B	10	60
C	10	75

Source: by the author.

3. Results and discussion

3.1 Pore morphology

Figure 2 shows SEM micrographs of the surface (a,b) and cross-section (c,d) of ma-PS layers formed in n-type silicon, i.e. samples A and C, respectively. Without pre-structuring, pores grow randomly on a flat wafer surface. The growth of random pores is usually preceded by some nucleation and redistribution phases (Fonthal et al., 2011). In the nucleation phase, the silicon surface is only homogeneously etched. At the end of the nucleation phase, a rough surface with high density shallow etching pores (pits) is formed.

During the redistribution phase, some of these small pores developed to macropores, while others died. It has been shown that the nucleation of the pores depends on the applied anodic voltage and etching temperature, as well as on the doping density. For low-doped n-type wafers, larger etching times are usually needed to achieve well-developed pores (Parimi, Tadigadapa, Yetter, 2014).

3.2 Electrical characterization

Figure 3 shows the dark I – V characteristics of metal/ma-PS/n-Si/Al diode, with Al-Ag and Ag top contacts respectively, in the range of ± 2 V at room temperature.

We have found that the dark I – V behavior of the ma-PS/n-Si structure corresponds to the classical diode behavior with rectifying factors of 3-4 orders of magnitude at ± 2 V.

Figure 3 shows the electrical model that describes the electrical behavior of the metal/ma-PS/n-Si/Al diodes. It can be represented by means of the following equation:

$$I = I_o\left\{\exp\left(\left(V - Vb\right)\Big/\eta * Vt\right) - 1\right\} + \frac{\left(V - Vb\right)}{R_p} = \frac{Vb}{R_S} + \left(\frac{Vb}{R_r}\right)^m \quad (1)$$

where *Io* is the dark saturation current,η is the ideality factor, *Vt* is the thermal voltage and *RS, RP* are the series and shunt resistance, respectively and Rr, m are the Space Charge Limit Current (SCLC) parametric (Balagurov et al., 2001) (m=1 (ohmic mechanism); m=2 (SCLC mechanism)).

For all the analysed samples, we obtained that this model presents an ideality factor value of η ~ 4,2, a high value of the series resistance RS ~ 5x103 Ω and a shunt resistance of RP ~ 7x106 Ω, The SCLC parameters Rr and m, 4,8 VA-1/m and 2, respectively.

Figure 2. SEM micrographs of (a,b) ma-PS surface and (c,d) the cross-section of the ma-PS layers for n type wafers etched for sample A and C

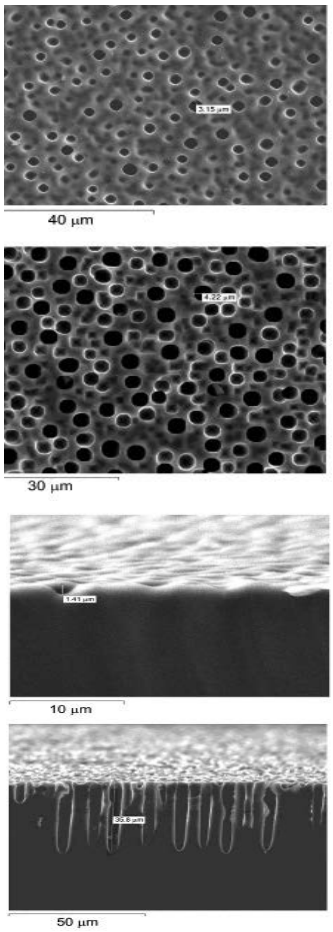

Source: by the author

Figure 3. Experimental dark I-V characteristic of metal/ma-PS/n-Si/Al diode for the sample C

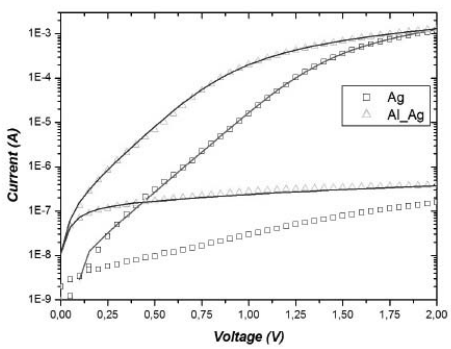

Source: by the author

Figure 4. Electrical model of the metal/ma-PS/n-Si/Al diode.

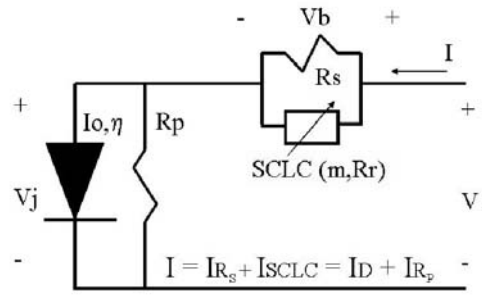

Source: by the author

3.3 Optical characterization of ma-PS layers

We performed reflectivity measurements of the formed ma-PS layers in order to determine their suitability as antireflection coatings. The monochromatic light falls onto the sample at an angle of 45º from the normal surface. The reflected light is recollected by a lens and projected on a silicon photodiode. Each sample was studied in the wavelength range from 200 to 1100 nm. The normalized reflectivity coefficient was determined as the ratio between the reflectivity measured for each ma-PS sample and the reflectivity measured from a bare silicon wafer. .

Figure 5. (a) Spectral measurement system ARC and (b) diagram of the different regions where light penetrate on the ma-PS surface in the spectral measurements

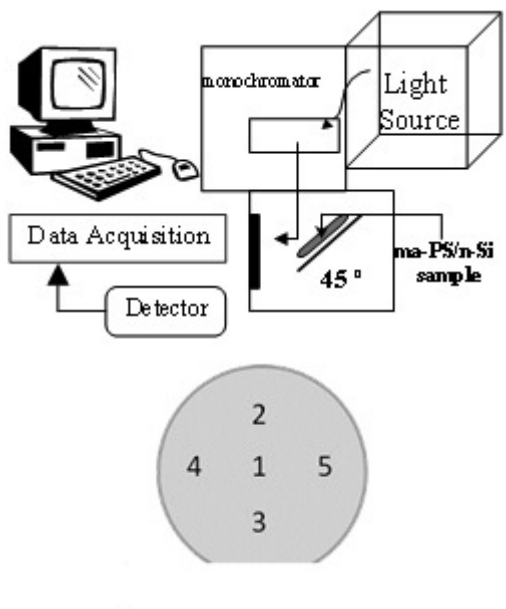

Source: by the author.

Figure 6a shows the normalized reflectivity for the sample A. In this sample we obtained very small holes, because this time is the minimum time in the electrochemical process conditions for ma-PS formation. Due to this, the normalized reflectivity values are relatively large (in the range of 20% - 50%). A great dispersion in the normalized reflectivity values for the different regions indicates non-homogeneity related to different depths of the pores in the crystalline silicon.

By increasing the etching time 15 min (Figure 6b) (sample B), we observed a lower dispersion in the different regions of the structure. The normalized reflectivity values are below 25%. This lower reflectivity shows a better uniformity in the pore formation, as well as a greater pore depth for each measured region than in the first sample.

Further increasing of the etching time by 15 min (sample C) it increases the porosity in the ma-PS surface, which improving the light absorption. As can be seen from Figure 6c, the normalized reflectivity presents the lowest values of about 10% with respect to the previous samples.

This seems to indicate that a critical depth exists in the formed pores, because when the etching time is increased, if possible it produces the electro-polished effect over the Si wafer. The normalized reflectivity value does not vary in the different regions, due to the uniformity stabilization of the formed holes in the ma PS/n-Si diode.

Figure 6. Normalized reflectivity spectrum of the ma PS/n Si/Al diode for different regions of the wafer and etching time: (a) 45, (b) 60 and (c) 75 min

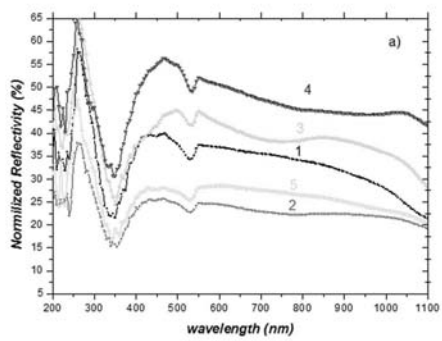

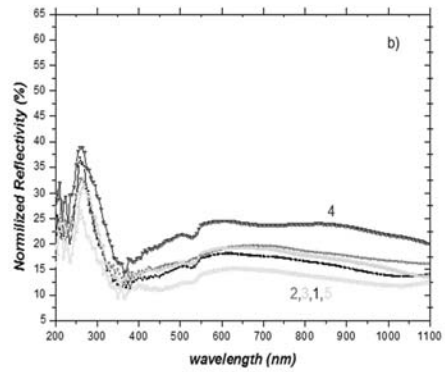

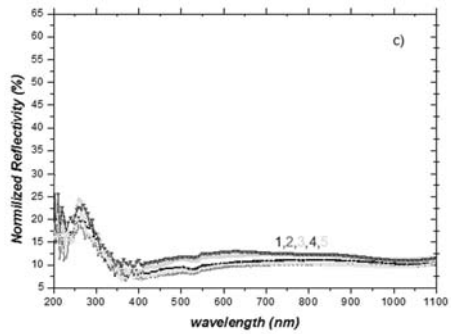

Source: by the author

4. Conclusions

We have measured the dark I – V characteristics of Al-Ag and Ag top contact in the ma-PS/n-Si structures. We observed that the current – voltage behavior of the junction of ma-PS on the n-Si follows the classical diode behavior with rectifying factors of 3-4 order.

We have obtained a relationship between the HF etching time of the wafer surface and the optical properties for the different samples. By increasing the etching time, the normalized reflectivity has been improved (values under 10% and lower dispersion). A critical depth exists of the formed pores, which minimizes the dispersion in the different regions for each sample.

Acknowledgements

The authors would like to thank Dr. A. Rodriguez (Universitat Politècnica Catalunya) and Dr. J. Pallarès (Universitat Rovira i Virgili) for their support in this investigation. This work was supported by the Universidad Autónoma de Occidente (UAO) under Project No. 08INTER-92.

References

AbdRahim, A. F., Hashim, M. R. & Ali, N. K. (2011). Physica B, 406, 1034.

Balagurov, L. et al. (2001). Appl. Phys., 90, 9, 4543.

Chen, C. W. et al. (2015). IEEE J. Photovoltaics, 5, 1, 123.

Ernst, M. et al. (2013). Energy Procedia, 38, 910.

Fonthal, F. & Chavarria, M. (2011). Physica Stat. Sol. C, 8, 6, 1913.

Fonthal, F., Torres, I. & Rodríguez, A. (2011). Mater. Sci: Mater. Electron., 22, 895.

Kanungo, J., Maji, S., Saha, H. & Basu, S. (2009). Solid-State Elect., 53, 663.

Ou, W., Zhao, L., Li, Z., Diao, H. & Wang, W. (2012). Int. J. Mater. and Mechanics Eng., 1, 1.

Parimi, V. S., Tadigadapa, S. A. & Yetter, R. A. (2014). Chem. Phys. Lett., 609, 129.

Salman, K. A., Hassan, Z. & Omar, K. (2012). Int. J. Electrochem. Sci., 7, 1, 376.

Xiao, S. H., Wang, R. H. & Bao, Y. J. (2012). Funct. Mater., 43, 3, 338.